Relationship between RPE and choriocapillaris in age-related macular degeneration

D. Scott McLeod, **Rhonda Grebe**, **Imran Bhutto**, **Carol Merges**, **Takayuki Baba**, and **Gerard A. Lutty**[*]

Wilmer Ophthalmological Institute, Johns Hopkins Hospital, Baltimore, MD, 21287

Abstract

Purpose—The purpose of this study was to examine the relationships between choriocapillaris (CC) and retinal pigment epithelial (RPE) changes in age-related macular degeneration (AMD). Morphological changes in the RPE/choriocapillaris complex were quantified in dry and wet forms of AMD and the results compared to with aged control eyes without maculopathy.

Methods—Postmortem choroids from 3 aged control subjects, 5 geographic atrophy (GA) subjects and 3 wet AMD subjects were analyzed using a semi-quantitative computer-assisted morphometric technique developed to measure percent RPE and CC areas in choroidal whole mounts incubated for alkaline phosphatase activity. The tissues were subsequently embedded in methacrylate and sectioned to examine structural changes.

Results—There was a linear relationship between the loss of RPE and CC in GA. A 50% reduction in vascular area was found in regions of complete RPE atrophy. Extreme constriction of remaining viable capillaries was found in areas devoid of RPE. Adjacent to active choroidal neovascularization (CNV) in wet AMD, CC dropout was evident in the absence of RPE atrophy resulting in a 50% decrease in vascular area. Lumenal diameters of the remaining capillaries in wet AMD eyes were similar to controls.

Conclusions—The primary insult in GA appears to be at the level of the RPE and there is an intimate relationship between RPE atrophy and secondary CC degeneration. CC degeneration occurs in the presence of viable RPE in wet AMD. The RPE in regions of vascular dropout are presumably hypoxic, which may result in an increase in VEGF production by the RPE and stimulation of CNV.

Keywords

age-related macular degeneration; geographic atrophy; choriocapillaris; retinal pigment epithelium; choroidal neovascularization

---

[*]Corresponding author: Gerard A. Lutty, PhD, G. Edward and G. Britton Durell, Professor of Ophthalmology, Wilmer Ophthalmological Institute, 170 Woods Research Building, Johns Hopkins Hospital, 600 North Wolfe St., Baltimore, MD 21287-9115. galutty@jhmi.edu.

INTRODUCTION

Age-related macular degeneration (AMD) is the leading cause of severe vision loss in patients above the age of 50 in industrialized countries. Despite the high prevalence, the etiology of AMD remains largely unknown. Clinically and histologically, AMD is generally classified into two major subtypes: dry or nonexudative AMD of which geographic atrophy (GA) is a severe form, and wet or exudative AMD. Dry AMD progresses more slowly and manifests with drusen, geographic or focal atrophy of the retinal pigment epithelium (RPE), and photoreceptor dysfunction and degeneration. Wet AMD, on the other hand, is more debilitating and often develops after early dry AMD. The key feature of wet AMD is choroidal neovascularization (CNV), the growth of new blood vessels from the choroid into the region underlying the RPE or extending into the subretinal space. In general, AMD pathology is characterized by degeneration involving the retinal photoreceptors, retinal pigment epithelium, Bruch's membrane, and choroidal capillaries.

Two different hypotheses have evolved regarding the pathogenesis of AMD: 1) RPE atrophy causes secondary choriocapillaris loss and photoreceptor degeneration; 2) choroidal vascular insufficiency results in dysfunction of the RPE and photoreceptor degeneration. Both of these events would lead to severe vision loss. The RPE and choriocapillaris share a mutualistic relationship. If one of the components is pathologic or compromised, either or both may become dysfunctional and/or degenerate. Experimental studies of selective destruction of the RPE by administration of sodium iodate or mechanical debridement showed that degeneration or removal of RPE caused atrophy of the choriocapillaris.[1–6] These changes, not only affect perfusion of the choriocapillaris, but also appear to compromise blood flow in the large choroidal vessels.[7] Changes in choriocapillaris perfusion after RPE removal may involve loss of RPE-derived trophic factors that maintain the integrity of the endothelium, leading to choriocapillaris atrophy.[4, 8] Studies have shown that basic fibroblast growth factor (bFGF), vascular endothelial growth factor (VEGF), endothelin-1, and insoluble molecules in the extracellular matrix produced by RPE act as survival factors for choroidal endothelial cells specifically and vascular endothelial cells in general.[9–14]

The role of hemodynamic changes, ischemia, and oxidative stress in AMD has been long recognized.[15–17] It has been hypothesized that AMD, stroke and cardiovascular disease may share a common pathogenesis. The potential link between AMD and vascular disease was recently highlighted in data from two large US studies.[18, 19] Oxidative stress, has been implicated in the pathogenesis of both AMD and vascular disease and may be the potential mechanism linking these two diseases.[20] Systemic inflammation has also been identified as a risk factor for both AMD and cardiovascular mortality. There is a growing body of evidence linking AMD with cardiovascular disease, suggesting that a dysfunctional circulatory system may be a common denominator for both conditions.[21]

In this study, we quantified and correlated RPE atrophy and choriocapillaris degeneration in aged non-AMD postmortem eyes and in eyes with GA and exudative AMD. Additionally, we examined lumenal diameters, structural changes in Bruch's membrane as well as loss of fenestrations in choriocapillaris endothelium.

MATERIALS AND METHODS

Donor Eyes

Choroids from 3 aged control subjects, 5 GA subjects and 3 wet AMD subjects were analyzed (Table 1). Donor eyes were obtained from the National Disease Research Interchange (NDRI) and through the help of Janet Sunness, MD and Carol Applegate (Greater Baltimore Medical Center, Baltimore, MD). Mean ages were 78 yrs (+/− 7.2) for controls, 83 yrs (+/− 9.7) for GA and 80.6 yrs (+/− 3.5) for wet AMD specimens. The eye banks provided the patient's age, sex, cause of death, brief ocular history (if available), brief medical history, and postmortem interval. Table 1 presents the characteristics of each subject used in this analysis. All donors were Caucasian. The diagnosis of AMD was made by reviewing ocular medical history (if available) and by postmortem gross examination of the posterior eyecups. The protocol of the study adhered to the tenets of the Declaration for Helsinki regarding research involving human tissue and was approved by the Johns Hopkins Medicine Institutional Review Boards.

Tissue preparation

The globes were opened at the limbus, anterior segments removed and eyecups examined using a stereomicroscope (Zeiss Stemi 2000, Carl Zeiss, Inc., Thornwood, New York). Gross images were obtained with a digital microscope camera (Micropublisher, QImaging) and imported via a plug-in into Adobe Photoshop CS3 (Adobe Systems Inc. San Jose, CA) on a MacPro computer (Apple, Cupertino, CA). The globes were examined and photographed using both epi-illumination and retro- or trans-illumination. Epi-illumination was used to view pigmentary changes in retina, and scarring associated with subretinal CNV. Trans-illumination accentuated hyper- and hypo-pigmentation, allowing us to clearly define the area of RPE atrophy. Two of the five GA eyes were clinically documented by Janet Sunness, M.D. (GBMC, Baltimore, MD), and the others diagnosed as GA because they had a clearly defined area of RPE atrophy that was centered on the fovea (Table 1). Wet AMD was diagnosed by the presence of scarring in the epi-illuminated globes or by the presence of CNV in the tissue after alkaline phosphatase incubation in the absence of a clearly demarcated area of RPE atrophy. The retinas were then excised from the eyecups and processed for ADPase flat-embedding[22] and will be the subject of a subsequent study. The choroids, with RPE intact, were imaged, dissected away from sclera, fixed and incubated for alkaline phosphatase (APase) activity as described previously.[23, 24]

After incubation, the choroids were washed and postfixed in 2% paraformaldehyde in 0.1 M cacodylate buffer, pH 7.2, at 4°C before being partially bleached in 30% hydrogen peroxide at 4°C. The tissue was inspected microscopically every two or three days during the bleaching process to ensure that some pigment remained visible. Bleaching was halted when the RPE pigment turned a light tan color and permitted visualization of the underlying APase$^+$ choroidal vasculature. The choroids were washed extensively and stored in 2% paraformaldehyde in 0.1 M cacodylate buffer, pH 7.2, at 4°C until being processed further.

Wet choroids were placed on slides and several radial cuts made in the tissue to allow for flattening. The flat preparations were initially imaged on a stereomicroscope using the

system descibed above. The submacular choroid, including the entire posterior pole, was trimmed from the tissue after obtaining low magnification transilluminated and epi-illuminated images.

Morphometric Analysis

The wet excised APase-incubated choroid was placed on a slide with the RPE closest to the objective, coverslipped under buffer and imaged at higher magnification using the digital color microscope camera on a Zeiss photomicroscope (Carl Zeiss, Inc., Thornwood, New York). RGB images (2048 × 1536 pixels) comprising areas of choroid equal to 1 mm^2 in area were captured using a Micropublisher digital camera (QImaging) and imported into Adobe Photoshop CS3 via plug-in. Two different types of illumination were used for imaging each field. Transmitted light from the microscope base was used to image viable blood vessels because it provided excellent visualization of the blue APase reaction product. Fiber optic cables were used to epi-illuminate and image viable RPE because it highlighted the partially bleached melanin granules within the cells. Images were captured and imported directly into Adobe Photoshop CS3.

Using the color range command of the Photoshop select menu, the blue APase staining was sampled using the eyedropper tool and vessels automatically selected in transmitted light images (Figure 1). Segments of vessels not selected using the eyedropper were added using the magic wand tool while holding the shift key. This selection technique allowed us to digitally isolate the blue choroidal vessels from other colored features within the image. This method, therefore, sampled both large and small blood vessels in a field. By selecting the tan color of the semi-bleached pigment in reflected light images, the same process was used to digitally isolate the RPE (Figure 1). The blood vessel selection and the RPE selection were then copied and pasted into new RGB documents and then converted to grayscale. The image size of the new documents was reduced to 640 × 480 pixels, saved as TIFF formats and subsequently imported into ImageJ software (Rasband, W.S., ImageJ, U. S. National Institutes of Health, Bethesda, Maryland, USA, http://rsb.info.nih.gov/ij/, 1997–2008.). Thresholding was performed and images were converted to binary. Percent vascular area (VA) or percent RPE area was measured on binary images (black vessels or RPE on a white background) using the "compute percent black and white" command in the measurement macros. This process was repeated for each field to be analyzed within the excised choroidal tissue. Prior to thresholding, grayscale images were saved to disk and used to make morphometric measurements of choriocapillaris diameters. For aged controls, this analysis was done in the submacular region. In GA eyes, submacular areas with RPE atrophy, areas at the border of atrophic and nonatrophic RPE (border zone), and areas with no RPE atrophy were measured. There were a few GA eyes with CNV but they were not included in the CNV analysis because they were very small in size and only consisted of several large blood vessels, i.e. they were not a neovascular network. In wet AMD specimens, regions outside of CNV formations in the submacular choroid were analyzed.

Capillary diameters were measured using the measuring tool in ImageJ on calibrated grayscale images. A minimum of 15 capillaries, in at least 3 fields of each region of interest

were determined. Only the portion of the capillary distant from any branches, bifurcations, or arteriolar or venular connections was measured.

After completing the wet preparation analysis, some pieces of the choroidal tissues containing regions of interest were flat embedded in glycol methacrylate (JB-4, Polysciences Inc., Warrington, PA, USA) as described previously and sectioned for further histologic analysis.[23, 24] Sections were stained with periodic acid Schiff's (PAS) and hematoxylin or hematoxylin and eosin (H&E).

Transmission Electronic Microscopy (TEM)

Tissues from 1 aged control (case #1) and 2 GA subjects (cases #4 & 5), were fixed overnight in 2.5% glutaraldehyde/2% paraformaldehyde in 0.1M cacodylate buffer pH 7.3 before washing in 0.05M cacodylate buffer and postfixed in1% OsO4 in 0.05 M cacodylate buffer for 90 min. Tissue was dehydrated in a series of graded ethanols (ETOH) (50, 70, 80, 95, and 100%) and then stained with 1% uranyl acetate in 100% ETOH. The tissue was placed in propylene oxide twice for 15 min each time, and then was kept overnight in 1:1 propylene oxide to resin mixture. The tissue was then infiltrated in 100% LX112 resin (Ladd Research Industry, Burlington, VT) for 4–6 hours under vacuum and finally embedded in a final change of 100% LX112 resin and polymerized at 60°C for 36–48 hours. Ultrathin sections were cut with a Leica Ultramicrotome UCT (Leica Microsystems, Wetzlar, Germany), stained with uranyl acetate and lead citrate and analyzed with a H7600 transmission electron microscope (Hitachi, Tokyo, Japan).

Statistical analysis

Data are reported as means +/− standard error of the mean. Statistical evaluation of the data involved calculating probability values using the Student's t-test for two samples assuming unequal variances. A p-value of 0.05 or less was considered significant.

RESULTS

Percent RPE and Percent Vascular Area

In aged control eyes, the submacular RPE was relatively homogeneous and uniform in size and pigmentation with a typical cobble-stone like morphology (Figure 2). The RPE coverage was 95.3 +/− 4.2% (Figure 3). The submacular choroidal vasculature was intensely stained for APase and appeared normal morphologically with regular branchings and freely interconnecting capillaries (Figure 2B). Measurements demonstrated that the vascular area was 79.6 +/− 3.8% (Figure 3). In GA subjects (Figure 4), there was a well-defined area of submacular RPE atrophy and degenerative changes in choriocapillaris. Outside the area of atrophy (Figure 5A, D, G &J), the RPE appeared somewhat mottled and in some cases had scattered small whitish drusen (Figure 5A). The choriocapillaris had normal APase activity and appeared relatively normal morphologically in areas without RPE atrophy (Figure 5G). Measurements obtained from non-atrophic regions (approximately one mm from the border of atrophic and nonatrophic areas) revealed that the RPE coverage was 92.32 +/− 3.24% and the vascular area was 72.26 +/− 4.8%, which was not significantly different from control subjects (%RPE p=0.292, %VA p=0.067) (Figure 3). At the border of atrophy (Figure 5B, E,

H & K), the remaining intact RPE cells were hypertrophic and some cells appeared hyper-pigmented. The choriocapillaris had reduced interconnecting segments and was attenuated in areas of RPE atrophy. In these regions, the percentage of RPE coverage was 38.1 +/− 5.8% and the vascular area was 52.3 +/− 3.3% which was significantly less than nonatrophic regions in GA choroids (%RPE p< 0.0001, %VA p=0.0001). Within the regions of atrophy (Figure 5C, F, I&L), only a few scattered RPE cells remained and the RPE coverage was 1.8 +/− 3.9% (Figure 3). The choriocapillaris was highly attenuated and had reduced branchings with few interconnecting segments (Figure 5I&L). Vascular area was 38 +/− 5.7%, which was significantly less than border regions (p=0.0013) of GA eyes (Figure 3).

In wet AMD choroids (Figure 6), measurements were made from binary images 1 mm peripheral to CNV (Figure 7). The percentage of RPE coverage in these regions was 95.9 +/− 1.8% and the vascular area was 39.6 +/− 15.9%. The decrease in vascular area was evident well beyond the submacular region and in one case extended peripherally 10 mm from the CNV into equatorial choroid (Figure 6C). The more distant from the CNV, however, the greater the percent vascular area. Compared with aged control eyes (Figure 8), wet AMD eyes had no significant changes in RPE coverage outside the area of CNV (P=0.85). However, the percent vascular area in these regions was significantly reduced reflecting loss of interconnecting capillary segments in these regions immediately in advance of the CNV (p=0.009).

Capillary Diameters

Mean capillary diameters (Figure 9) were 14.6 +/− 1.1 μm in aged control eyes. In GA eyes, capillary diameters were 13.9 +/− 1.4 μm in nonatrophic regions and not significantly reduced compared to aged controls (p=0.4434). Capillary diameters were 10.34 +/− 0.7 μm in border regions and 7.9 +/− 1.2 μm in regions of atrophy. Compared to capillaries in nonatrophic regions, capillary diameters at the border were significantly reduced (p=0.001). Similarly, capillary diameters in the atrophic region were significantly reduced compared to those at the border (p=0.007). Capillary diameters in wet AMD eyes were 13.9 +/− 0.4 μm. There was no significant difference in diameters between the aged control and the viable capillaries in wet AMD eyes 1 mm outside the area of CNV (p=0.348).

Histology

Cross sections through the three regions analysed in GA eyes confirmed the observations made in flat preparations (Figure 10). In nonatrophic regions, the choriocapillaris displayed broad lumens, with APase positive endothelial cells. The lumens often contained serum APase. The RPE had a normal structure, with rounded nuclei and melanocytes concentrated in their apical cytoplasm. In border regions, many capillaries were withdrawn from the intercapillary pillars, RPE were increased in height and basal laminar deposits were present (Figure 10H, open arrow). Capillaries in regions devoid of RPE showed severe degenerative changes and, in some cases, only remnants of basement membrane material remained. The remaining viable capillaries were extremely constricted, being withdrawn from the surrounding intercapillary pillars that had increased staining with PAS. Bruch's membrane was generally devoid of deposits or drusen in atrophic regions.

In wet AMD eyes (Figure 11), sections from regions temporal to submacular CNV that showed good staining of vessels in flat preparations, revealed broad capillary lumens with endothelial cells and pericytes. In some subjects the lumen contained serum APase. The RPE were relatively uniform in size and Bruch's membrane was unremarkable. In areas closer to the CNV, the capillary dropout that was observed in flat preparations was confirmed. While some capillaries were obviously patent because of the presence of serum APase within their lumens, others were degenerated with only remnants of basement membrane material present. The adjacent RPE were hypertrophic with a scalloped morphology and basal laminar deposits were present. Sections taken at the peripheral edge of CNV formations showed hypertrophic RPE overlying the growing tips of the blood vessels, basal laminar deposit and choriocapillaris dropout. Besides the changes associated with choriocapillaris, medium and large choroidal arteries in both dry and wet AMD eyes showed pathologic changes consistent with both hyaline and hyperplastic arteriolosclerosis (Figure 12).

Ultrastructure

Examination of TEM sections of an aged control eye demonstrated a thin endothelium with numerous fenestrations with single-layered diaphragms along the inner aspect of the choriocapillaris (Figure 13). Additionally, fenestrations were seen along the outer capillary wall as well but to a lesser degree. In GA eyes where RPE were present, fewer fenestrations per capillary were observed compared to control choroid. In border regions, the number of fenestrations was reduced even more and few if any were observed in regions of atrophy. In these areas, the inner aspect of the capillary endothelium was thickened and cytoplasmic loops were observed projecting into the lumenal space (Figure 14). Often these loops had fenestrations within them (Figure 14C) but were considered abnormal because they were not in a position where they would be functional. Fenestration counts made from 2 GA eyes revealed that areas with RPE had statistically significant higher numbers of fenestrations per capillary (6.53 +/− 0.996) than regions devoid of RPE (0.55 +/− 0.235) where few if any were observed (case #4 P=0.019, case #5 p=0.001).

DISCUSSION

Although limited in the number of eyes examined, this study demonstrates that there is a linear relationship in the loss of RPE and CC in GA. A 50% mean reduction in vascular area was found in regions of RPE atrophy compared to regions in GA eyes with RPE and in aged control eyes without maculopathy. We did not observe complete loss of choriocapillaris in areas of total RPE atrophy in any GA eyes, even though the atrophy had been documented clinically for 20 years prior to death in one patient. However, the surviving capillaries that remained in these regions were extremely constricted, being half of the diameter of capillaries where RPE were present. Moreover, we noted a loss of fenestrations in the endothelium of these constricted capillaries suggesting functional changes. Experimental studies have shown that RPE cell death precedes choriocapillaris atrophy[4, 6] and that destroying RPE causes loss of fenestrations.[2, 4] Presumably, this occurs because RPE constitutively produce factors like VEGF[25] that stimulate formation of fenestrations.[12] VEGF is also a potent vasodilator[26], endothelial cell survival factor[27] and induces

angiogenesis.[28] RPE cells in vitro have been shown to secrete VEGF basally (toward the choriocapillaris) and VEGF receptors are expressed on the choroidal endothelium facing the RPE layer in human.[29] Consistent with these observations and VEGF's known functions, it is reasonable to conclude that in GA where RPE have atrophied, the source of VEGF is removed and capillaries either constrict and lose fenestrations or degenerate and eventually atrophy. The clinical impression that areas of RPE atrophy in GA lack a choriocapillaris may be due to the extreme constriction of the surviving vascular segments and loss of fenestrations, so the dye filling of these segments is negligible and leakage through fenestrations does not occur.

The close association we observed between degenerating RPE and choriocapillaris suggests that at least in GA, RPE atrophy occurs first followed by choriocapillaris degeneration. The mechanism(s) of RPE degeneration in AMD is likely to be multifactorial with oxidative stress, environmental factors, intense light exposure and genetics all potentially involved. Oxidative stress has been proposed in AMD through several mechanisms[30, 31], including blue light-induced photochemically released oxidants that damage cells[32], cigarette smoke-related oxidants such as hydroquinone that alter Bruch's membrane[33], iron-induced oxidative damage to the outer retina[34], and possibly advanced glycation end products (AGEs) within Bruch's membrane.[35, 36] The lesions induced by oxidative injury may accumulate over time and trigger affected RPE cells to undergo apoptosis. If oxidative stress is involved in the etiology of AMD, then the aging process of RPE and the development of AMD might be prevented or delayed by increasing the antioxidant capacity of RPE. In support of this hypothesis, the Age-Related Eye Disease Study has demonstrated that a combination of antioxidants and zinc supplements, beyond what can be achieved through diet alone, reduced the risk of severe AMD and vision loss in humans.[37]

In this study, choriocapillaris dropout occurred in the three wet AMD specimens, without RPE atrophy in advance of CNV resulting in a 50% decrease in vascular area compared to aged control eyes. The theory that the choroidal vasculature plays a driving role in AMD development is well established. Duke-Elder suggested that most cases of AMD were due to sclerosis and obliteration of the choriocapillaris in the submacular area.[38] Later Friedman[39] proposed a hemodynamic model for AMD, which he later revised to a vascular model.[40, 41] This model suggests that AMD is a vascular disorder characterized by impairment of choroidal perfusion. It highlights the roles of the atherosclerotic process and blood pressure in the pathogenesis of the disorder. AMD shares common risk factors with cardiovascular disease and recent large clinical studies support that vascular factors may contribute to its pathogenesis. Studies demonstrate that persons with hypertension and atherosclerosis are more likely to have AMD.[42–45] Quantitative and qualitative ocular blood flow abnormalities have been consistently described in early and late AMD[46] and numerous studies have implicated ischemia as a primary stimulus for AMD.[15, 47–51] A vascular deficit in AMD is supported by previous histological findings that showed a reduction in the cross sectional area of the choriocapillaris in persons with AMD.[52, 53]

The driving mechanism for development of NV is hypoxia/ischemia. The presence of choriocapillaris atrophy in the vicinity of CNV has been reported previously.[23, 54] Melrose et al described a patient with choroidal nonperfusion underlying subretinal

neovascularization.[55] They suggested that chronic macular ischemia occurred secondary to choroidal blood flow impairment. Hayashi and de Laey using ICG angiography demonstrated watershed zones or areas of choroidal circulatory disturbance associated with CNV in AMD.[56] Our results support these previous findings and lend credence to the theory of a vascular basis for the development of at least the exudative form of AMD. The observed intimate association of CNV with viable RPE suggests that their presence and factors they produce are required for the growth and expansion of pathologic neovascularization.

In conclusion, despite the limited number of specimens analyzed, this study demonstrated that choriocapillaris degenerates in GA and exudative AMD, but the etiology of the two types of AMD may differ. RPE atrophy appears to be the initial insult in GA whereas choriocapillaris degeneration precedes RPE atrophy in wet AMD. The mutualistic relationship between choriocapillaris and RPE is ultimately lost in both forms of AMD.

Acknowledgments

References

1. Hayashi A, Majji AB, Fujioka S, Kim HC, Fukushima I, de Juan E Jr. Surgically induced degeneration and regeneration of the choriocapillaris in rabbit. Graefes Arch Clin Exp Ophthalmol. 1999; 237:668–677. [PubMed: 10459617]

2. Henkind P, Gartner S. The relationship between retinal pigment epithelium and the choriocapillaris. Trans Ophthalmol Soc U K. 1983; 103:444–447. [PubMed: 6589861]

3. Heriot WJ, Machemer R. Pigment epithelial repair. Graefes Arch Clin Exp Ophthalmol. 1992; 230:91–100. [PubMed: 1547975]

4. Korte GE, Repucci V, Henkind P. RPE destruction causes choriocapillary atrophy. Invest Ophthalmol Vis Sci. 1984; 25:1135–1145. [PubMed: 6480292]

5. Leonard DS, Sugino IK, Zhang XG, et al. Ultrastructural analysis of hydraulic and abrasive retinal pigment epithelial cell debridements. Exp Eye Res. 2003; 76:473–491. [PubMed: 12634112]

6. Leonard DS, Zhang XG, Panozzo G, Sugino IK, Zarbin MA. Clinicopathologic correlation of localized retinal pigment epithelium debridement. Invest Ophthalmol Vis Sci. 1997; 38:1094–1109. [PubMed: 9152229]

7. Ivert L, Kong J, Gouras P. Changes in the choroidal circulation of rabbit following RPE removal. Graefes Arch Clin Exp Ophthalmol. 2003; 241:656–666. [PubMed: 12883908]

8. Del Priore LV, Kaplan HJ, Hornbeck R, Jones Z, Swinn M. Retinal pigment epithelial debridement as a model for the pathogenesis and treatment of macular degeneration. Am J Ophthalmol. 1996; 122:629–643. [PubMed: 8909202]

9. Alon T, Hemo I, Itin A, Pe'er J, Stone J, Keshet E. Vascular endothelial growth factor acts as a survival factor for newly formed retinal vessels and has implications for retinopathy of prematurity. Nature Medicine. 1995; 1:1024–1028.

10. Karsan A, Yee E, Poirier GG, Zhou P, Craig R, Harlan JM. Fibroblast growth factor-2 inhibits endothelial cell apoptosis by Bcl-2-dependent and independent mechanisms. Am J Pathol. 1997; 151:1775–1784. [PubMed: 9403728]

11. Liu X, Ye X, Yanoff M, Li W. Extracellular matrix of retinal pigment epithelium regulates choriocapillaris endothelial survival in vitro. Exp Eye Res. 1997; 65:117–126. [PubMed: 9237872]

12. Roberts W, Palade G. Increased microvascular permeability and endothelial fenestration induced by vascular endothelial growth factor. J Cell Sci. 1995; 108:2369–2379. [PubMed: 7673356]

13. Shichiri M, Kato H, Marumo F, Hirata Y. Endothelin-1 as an autocrine/paracrine apoptosis survival factor for endothelial cells. Hypertension. 1997; 30:1198–1203. [PubMed: 9369276]

14. Watanabe Y, Dvorak HF. Vascular permeability factor/vascular endothelial growth factor inhibits anchorage-disruption-induced apoptosis in microvessel endothelial cells by inducing scaffold formation. Exp Cell Res. 1997; 233:340–349. [PubMed: 9194496]

15. Friedman E, Krupsky S, Lane AM, et al. Ocular blood flow velocity in age-related macular degeneration. Ophthalmology. 1995; 102:640–646. [PubMed: 7724181]

16. Grunwald J, Hariprasad S, DuPont J, et al. Foveolar choroidal blood flow in age-related macular degeneration. Invest Ophthalmol Vis Sci. 1998; 39:385–390. [PubMed: 9477998]

17. Kornzweig A. Changes in the choriocapillaris associated with senile macular degeneration. Ann Ophthalmol. 1977; 9:753–764. [PubMed: 911118]

18. Duan Y, Mo J, Klein R, et al. Age-related macular degeneration is associated with incident myocardial infarction among elderly Americans. Ophthalmology. 2007; 114:732–737. [PubMed: 17187863]

19. Wong TY, Klein R, Sun C, et al. Age-related macular degeneration and risk for stroke. Ann Intern Med. 2006; 145:98–106. [PubMed: 16847292]

20. Beatty S, Koh H, Phil M, Henson D, Boulton M. The role of oxidative stress in the pathogenesis of age-related macular degeneration. Surv Ophthalmol. 2000; 45:115–134. [PubMed: 11033038]

21. Hogg RE, Woodside JV, Gilchrist SE, et al. Cardiovascular disease and hypertension are strong risk factors for choroidal neovascularization. Ophthalmology. 2008; 115:1046–1052 e1042. [PubMed: 17953990]

22. Lutty GA, McLeod DS. A new technique for visualization of the human retinal vasculature. Arch Ophthalmol. 1992; 110:267–276. [PubMed: 1736877]

23. McLeod DS, Lutty GA. High resolution histologic analysis of the human choroidal vasculature. Invest Ophthalmol Vis Sci. 1994; 35:3799–3811. [PubMed: 7928177]

24. McLeod DS, Taomoto M, Otsuji T, Green WR, Sunness JS, Lutty GA. Quantifying changes in RPE and choriocapillaris in eyes with age-related macular degeneration. Invest Ophthalmol Vis Sci. 2002; 43:1986–1993. [PubMed: 12037009]

25. Adamis AP, Shima DT, Yeo KT, et al. Synthesis and secretion of vascular permeability factor/ vascular endothelial growth factor by human retinal pigment epithelial cells. Biochem Biophys Res Commun. 1993; 193:631–638. [PubMed: 8512562]

26. Tolentino MJ, McLeod DS, Taomoto M, Otsuji T, Adamis AP, Lutty GA. Pathological features of vascular endothelial growth factor-induced retinopathy in nonhuman primates. Am J Ophthalmol. 2002; 133:373–385. [PubMed: 11860975]

27. Benjamin LE, Keshet E. Conditional switching of vascular endothelial growth factor (VEGF) expression in tumors: induction of endothelial cell shedding and regression of hemangioblastoma-like vessels by VEGF withdrawal. Proc Natl Acad Sci U S A. 1997; 94:8761–8766. [PubMed: 9238051]

28. Esser S, Wolburg K, Wolburg H, Breier G, Kurzchalia T, Risau W. Vascular endothelial growth factor induces endothelial fenestrations in vitro. J Cell Biol. 1998; 140:947–959. [PubMed: 9472045]

29. Blaauwgeers HG, Holtkamp GM, Rutten H, et al. Polarized vascular endothelial growth factor secretion by human retinal pigment epithelium and localization of vascular endothelial growth factor receptors on the inner choriocapillaris. Am J Pathol. 1999; 155:421–428. [PubMed: 10433935]

30. Cai J, Nelson KC, Wu M, Sternberg P Jr, Jones DP. Oxidative damage and protection of the RPE. Prog Retin Eye Res. 2000; 19:205–221. [PubMed: 10674708]

31. Spaide RF, Armstrong D, Browne R. Continuing medical education review: choroidal neovascularization in age-related macular degeneration–what is the cause? Retina. 2003; 23:595–614. [PubMed: 14574243]

32. Margrain TH, Boulton M, Marshall J, Sliney DH. Do blue light filters confer protection against age-related macular degeneration? Prog Retin Eye Res. 2004; 23:523–531. [PubMed: 15302349]

33. Espinosa-Heidmann DG, Suner IJ, Catanuto P, Hernandez EP, Marin-Castano ME, Cousins SW. Cigarette smoke-related oxidants and the development of sub-RPE deposits in an experimental animal model of dry AMD. Invest Ophthalmol Vis Sci. 2006; 47:729–737. [PubMed: 16431974]

34. Dunaief JL. Iron induced oxidative damage as a potential factor in age-related macular degeneration: the Cogan Lecture. Invest Ophthalmol Vis Sci. 2006; 47:4660–4664. [PubMed: 17065470]

35. Tian J, Ishibashi K, Ishibashi K, et al. Advanced glycation end product-induced aging of the retinal pigment epithelium and choroid: a comprehensive transcriptional response. Proc Natl Acad Sci U S A. 2005; 102:11846–11851. [PubMed: 16081535]

36. Yamada Y, Ishibashi K, Ishibashi K, et al. The expression of advanced glycation end product receptors in RPE cells associated with basal deposits in human maculas. Exp Eye Res. 2006; 82:840–848. [PubMed: 16364296]

37. Age-related Eye Disease Study Research Group. A randomized, placebo-controlled, clinical trial of high-dose supplementation with vitamins C and E, beta carotene, and zinc for age-related macular degeneration and vision loss: AREDS report no. 8. Arch Ophthalmol. 2001; 119:1417–1436. [PubMed: 11594942]

38. Duke-Elder, S. System of Ophthalmology Diseases of the Uveal Tract. St. Louis: The C.V. Mosby Company; 1966. p. 608

39. Friedman E. A hemodynamic model of the pathogenesis of age-related macular degeneration. Am J Ophthalmol. 1997; 124:677–682. [PubMed: 9372722]

40. Friedman E. Age related macular degeneration. Update of the vascular model of AMD. Brit J Ophthalmol. 2004; 88:161–163. [PubMed: 14736760]

41. Friedman E. The pathogenesis of age-related macular degeneration. Am J Ophthalmol. 2008; 146:348–349. [PubMed: 18724980]

42. Hyman L, Schachat AP, He Q, Leske MC. Hypertension, cardiovascular disease, and age-related macular degeneration. Age-Related Macular Degeneration Risk Factors Study Group. Arch Ophthalmol. 2000; 118:351–358. [PubMed: 10721957]

43. Snow KK, Seddon JM. Do age-related macular degeneration and cardiovascular disease share common antecedents? Ophthalmic Epidemiol. 1999; 6:125–143. [PubMed: 10420212]

44. van Leeuwen R, Ikram MK, Vingerling JR, Witteman JC, Hofman A, de Jong PT. Blood pressure, atherosclerosis, and the incidence of age-related maculopathy: the Rotterdam Study. Invest Ophthalmol Vis Sci. 2003; 44:3771–3777. [PubMed: 12939290]

45. Vingerling JR, Dielemans I, Bots ML, Hofman A, Grobbee DE, de Jong PT. Age-related macular degeneration is associated with atherosclerosis. The Rotterdam Study. Am J Epidemiol. 1995; 142:404–409. [PubMed: 7625405]

46. Harris A, Chung HS, Ciulla TA, Kagemann L. Progress in measurement of ocular blood flow and relevance to our understanding of glaucoma and age-related macular degeneration. Prog Retin Eye Res. 1999; 18:669–687. [PubMed: 10438154]

47. Chen J, Fitzke F, Bird A. Functional loss in age-related Bruch's membrane change with choroidal perfusion defect. Invest Ophthalmol Vis Sci. 1992; 33:334–340. [PubMed: 1740363]

48. Feigl B. Age-related maculopathy-linking aetiology and pathophysiological changes to the ischaemia hypothesis. Prog Retin Eye Res. 2009; 28:63–86. [PubMed: 19070679]

49. Grunwald J, Hariprasad S, DuPont J. Effect of aging on foveolar choroidal circulation. Arch Ophthalmol. 1998; 116:150–154. [PubMed: 9488265]

50. Grunwald JE, Metelitsina TI, Dupont JC, Ying GS, Maguire MG. Reduced foveolar choroidal blood flow in eyes with increasing AMD severity. Invest Ophthalmol Vis Sci. 2005; 46:1033–1038. [PubMed: 15728562]

51. Pauleikhoff D, Chen J, Chisholm I, Bird A. Choroidal perfusion abnormality with age-related bruch's membrane change. Am J Ophthalmol. 1990; 109:211–217. [PubMed: 2301534]

52. Ramrattan RS, van der Schaft TL, Mooy CM, de Bruijn WC, Mulder PG, de Jong PT. Morphometric analysis of Bruch's membrane, the choriocapillaris, and the choroid in aging. Invest Ophthalmol Vis Sci. 1994; 35:2857–2864. [PubMed: 8188481]

53. Sarks JP, Sarks SH, Killingsworth MC. Evolution of geographic atrophy of the retinal pigment epithelium. Eye. 1988; 2:552–577. [PubMed: 2476333]

54. Gass, JD. Stereoscopic Atlas of Macular Diseases Diagnosis and Treatment. St. Louis: Mosby; 1997. p. 80

55. Melrose MA, Magargal LE, Goldberg RE, Annesley WH Jr. Subretinal neovascular membranes associated with choroidal nonperfusion and retinal ischemia. Ann Ophthalmol. 1987; 19:396–399. [PubMed: 2446561]

56. Hayashi K, de Laey JJ. Indocyanine green angiography of choroidal neovascular membranes. Ophthalmologica. 1985; 190:30–39. [PubMed: 2578633]
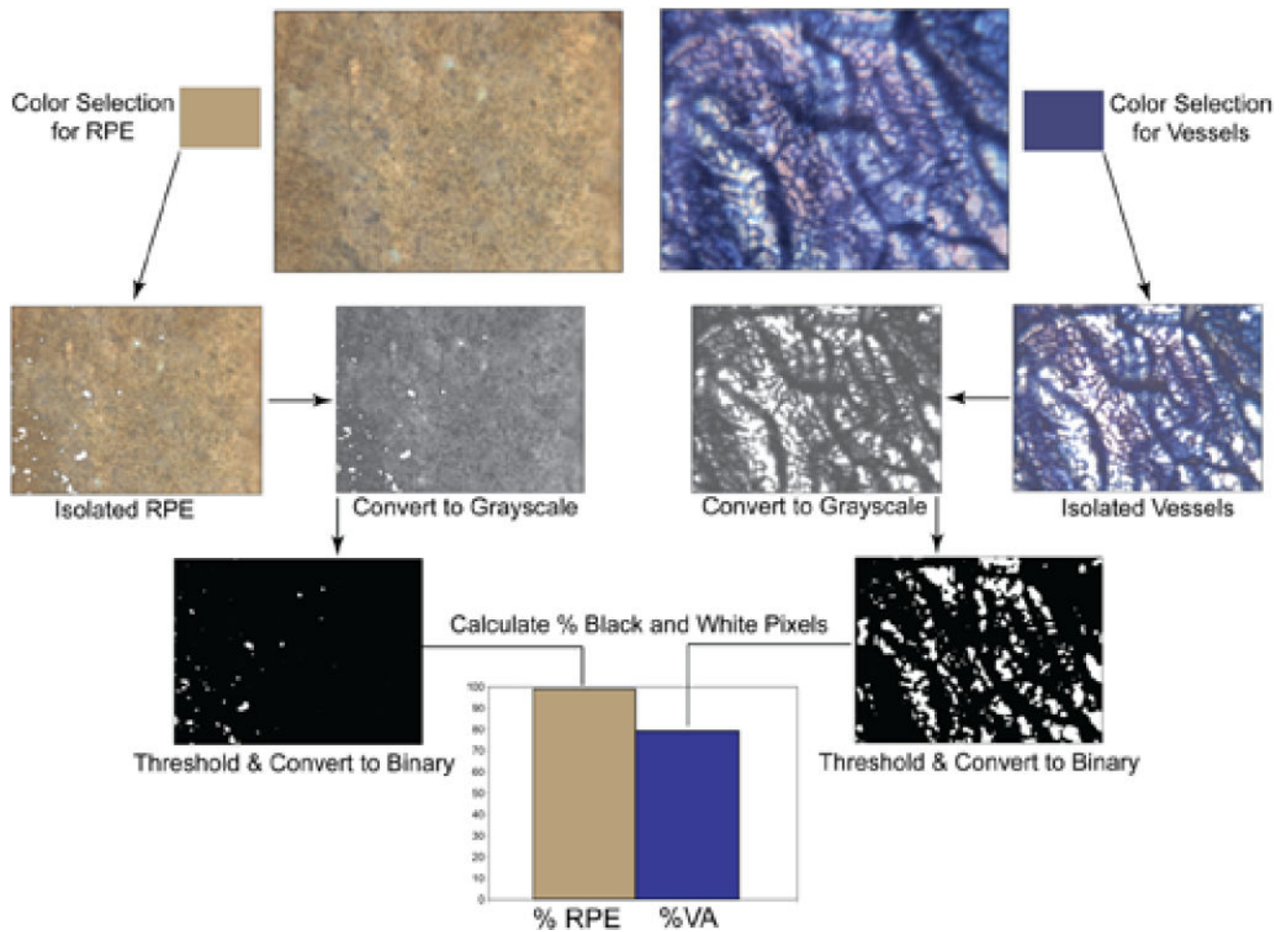
Figure 1.
Flow diagram showing the processing of images for determination of percent RPE or vascular area in a control subject (Case #3). Color selection was used to isolate the RPE (left) or vasculature (right), pixels copied and pasted into new images, converted to grayscale and thresholding was performed. The image was then converted to binary and imported into ImageJ where measurements were made using the "compute percent black and white" command in the measurement macros.
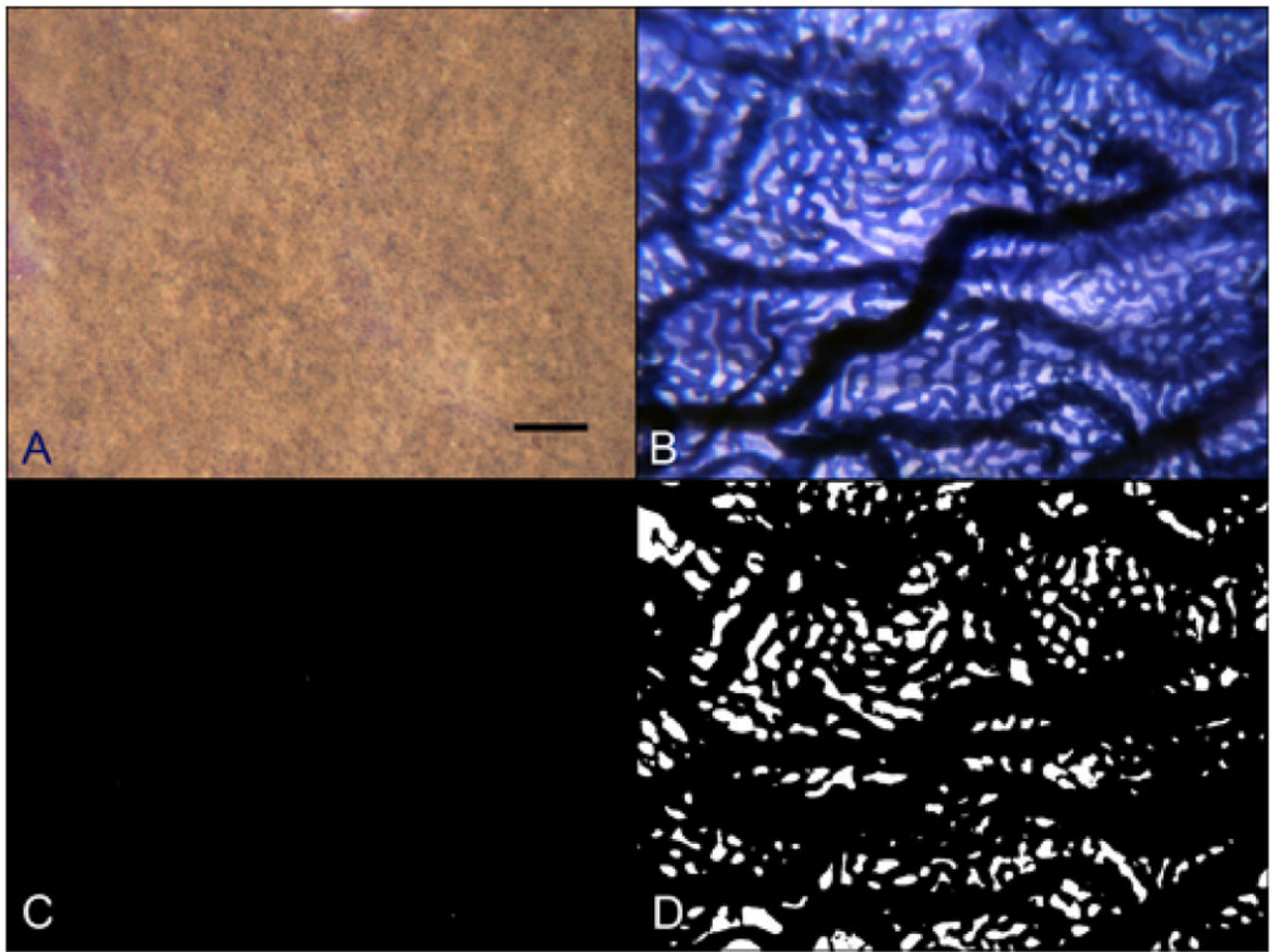
Figure 2.
Raw color images of RPE using epi-illumination (A) and APase stained choroidal vessels using transillumination (B) and converted binary images used to make final percent black and percent white determinations from a flat preparation of an 80 year-old Caucasian male aged control subject (Case #2). (scale bar = 100 μm)
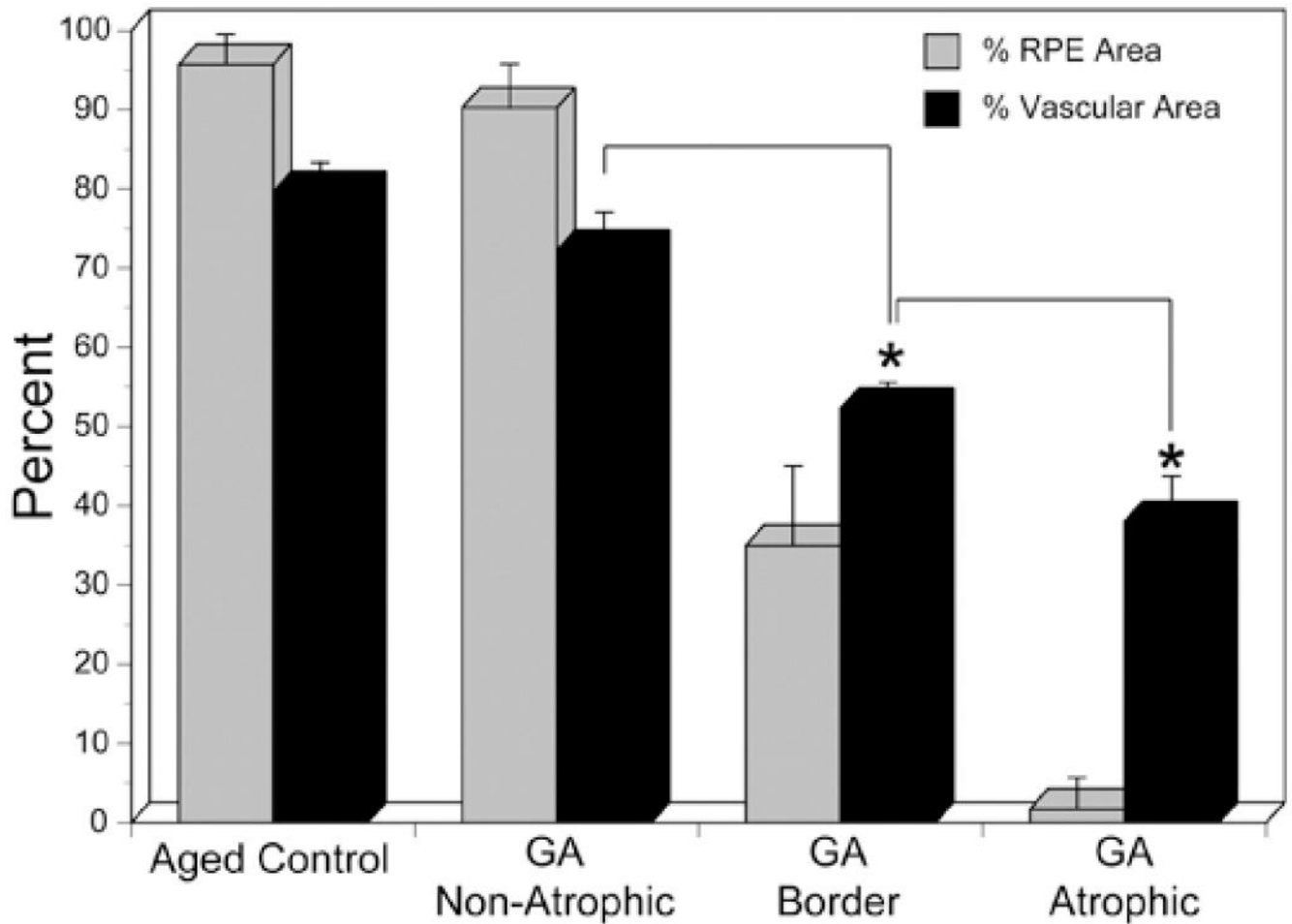
Figure 3.
Comparison of percent RPE area and percent vascular area in aged control subjects and in the three regions analyzed in geographic atrophy choroids (GA). There was no statistically significant difference between aged control and nonatrophic regions of GA eyes in terms of RPE area (p=0.292) or vascular area (p=0.067). However, in GA choroid, there was a statistically significant decrease in both RPE (<0.0001) and vascular area (p=0.0001) in the border region compared to the nonatrophic region (asterisk). Similarly, there was a significant decrease in the RPE area (<0.0001) and vascular area (p=0.0013) in the atrophic region compared to the border region (asterisk).
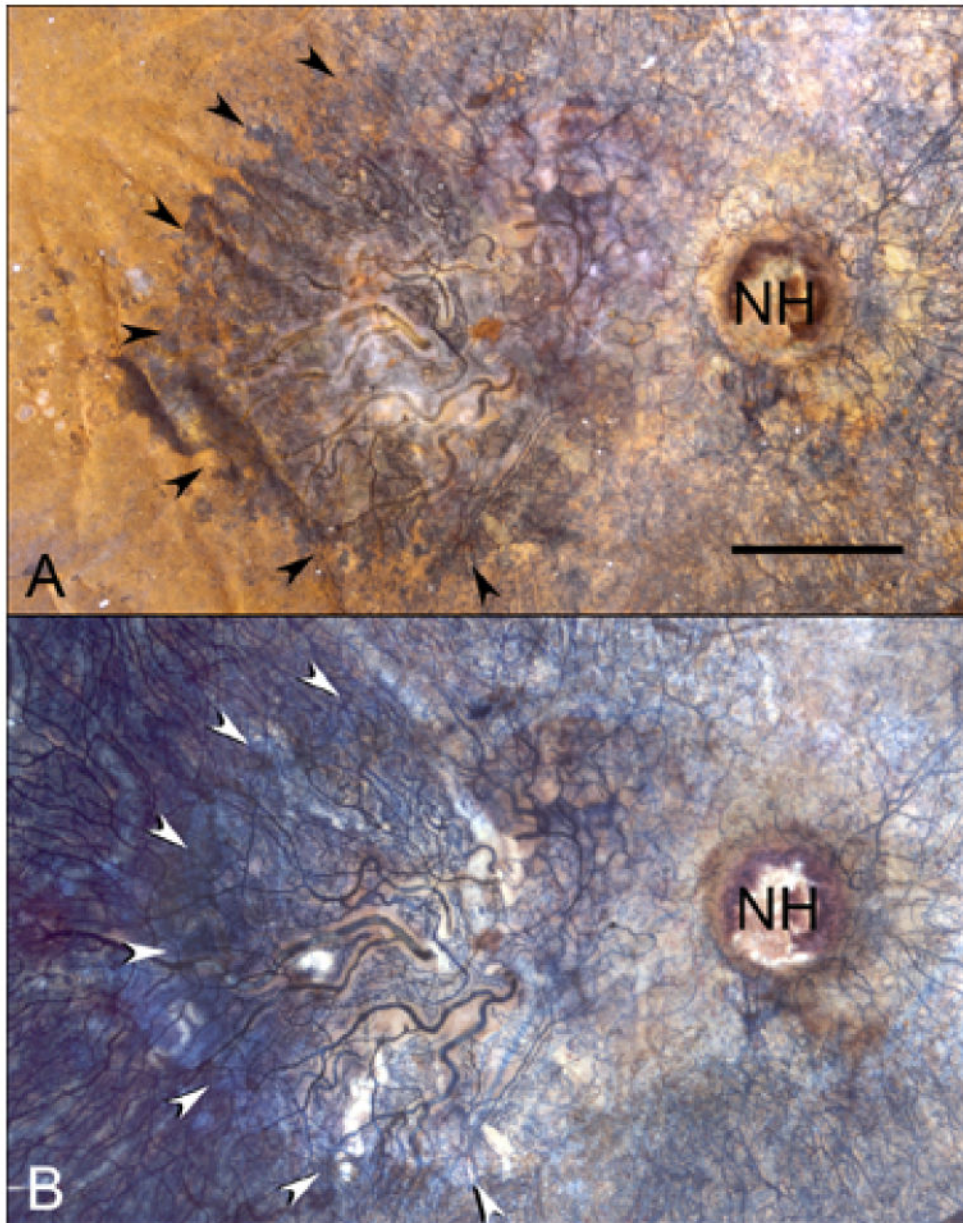
Figure 4.
APase choroid from an 88 year-old Caucasian male (Case #7) with a well-defined area of geographic atrophy (arrows) measuring 26.3 mm^2 is shown with epi-illumination (A) and transillumination (B). The optic nerve head is indicated (NH). (scale bar = 2mm)
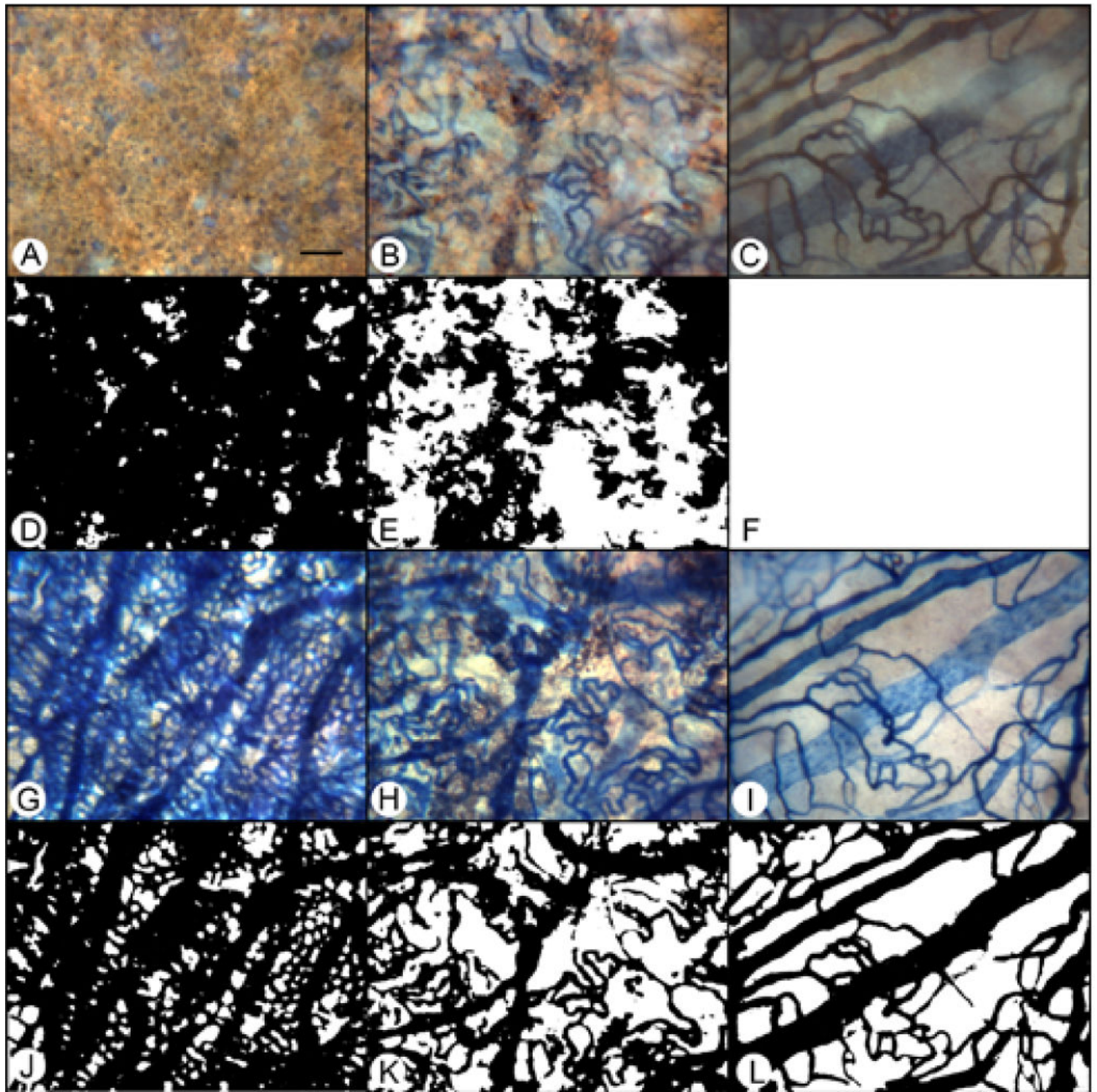
Figure 5.
APase choroid from a 79 year-old Caucasian male with GA (Case #8) showing nonatrophic (A,D,G,J), border (B,E,H,K) and atrophic region (C,F,I,L). Images captured with epi-illumination (A–C) highlight the RPE and were processed to make the binary images used to measure RPE area (D–F). The same three regions are shown with transillumination (G–I) along with the binary images used to measure percent vascular area (J–L). (scale bar = 100 μm)
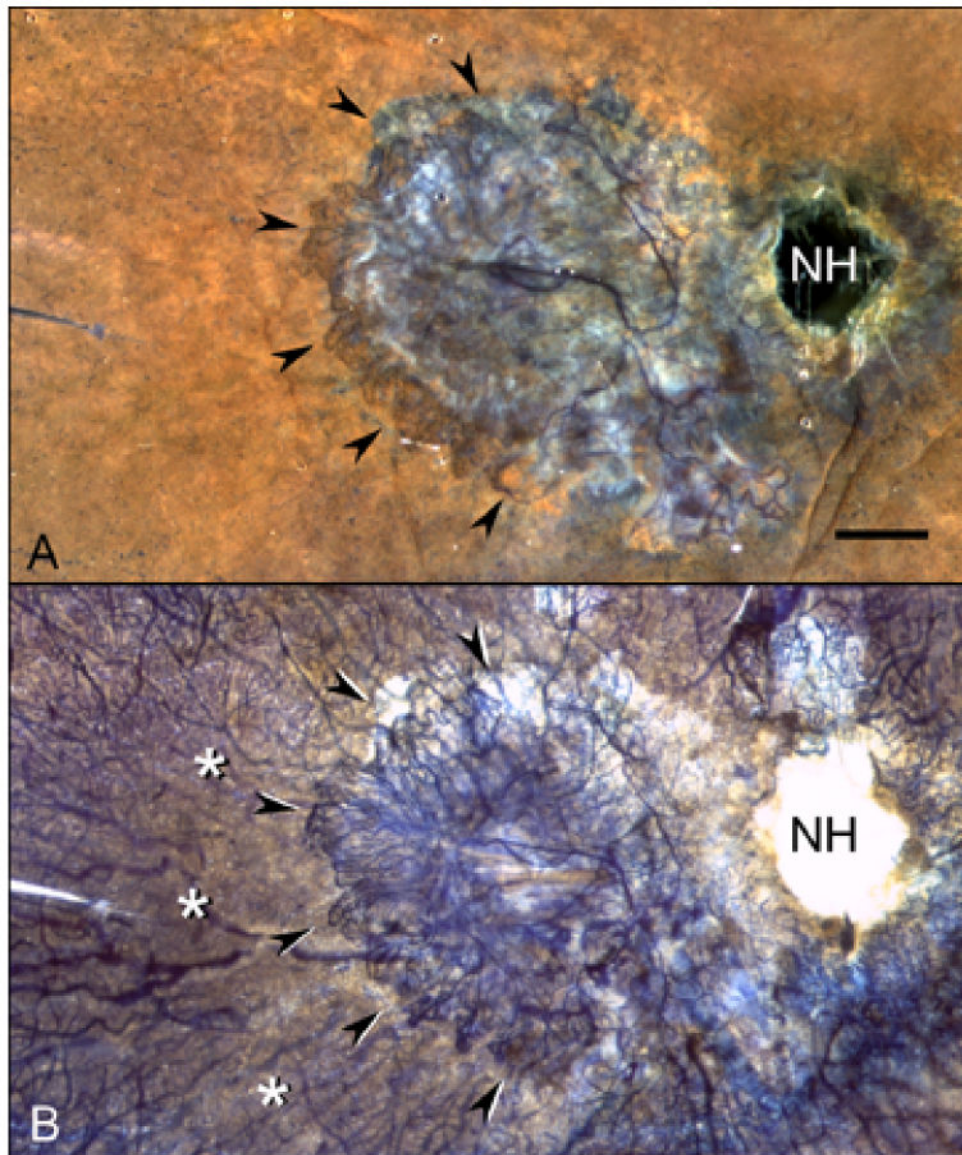
Figure 6.
APase choroid from an 81 year-old Caucasian female with wet AMD (Case #10). A submacular seafan-like CNV formation is shown (arrowheads) using epi-illumination (A) and transillumination (B). Areas of choriocapillaris dropout are located in advance of the CNV (asterisks). Percent RPE and vascular area measurements made in 2 mm intervals from the CNV (C) show that capillary dropout is present well beyond the extent of neovascularization. (NH = nerve head, scale bar = 2 mm)
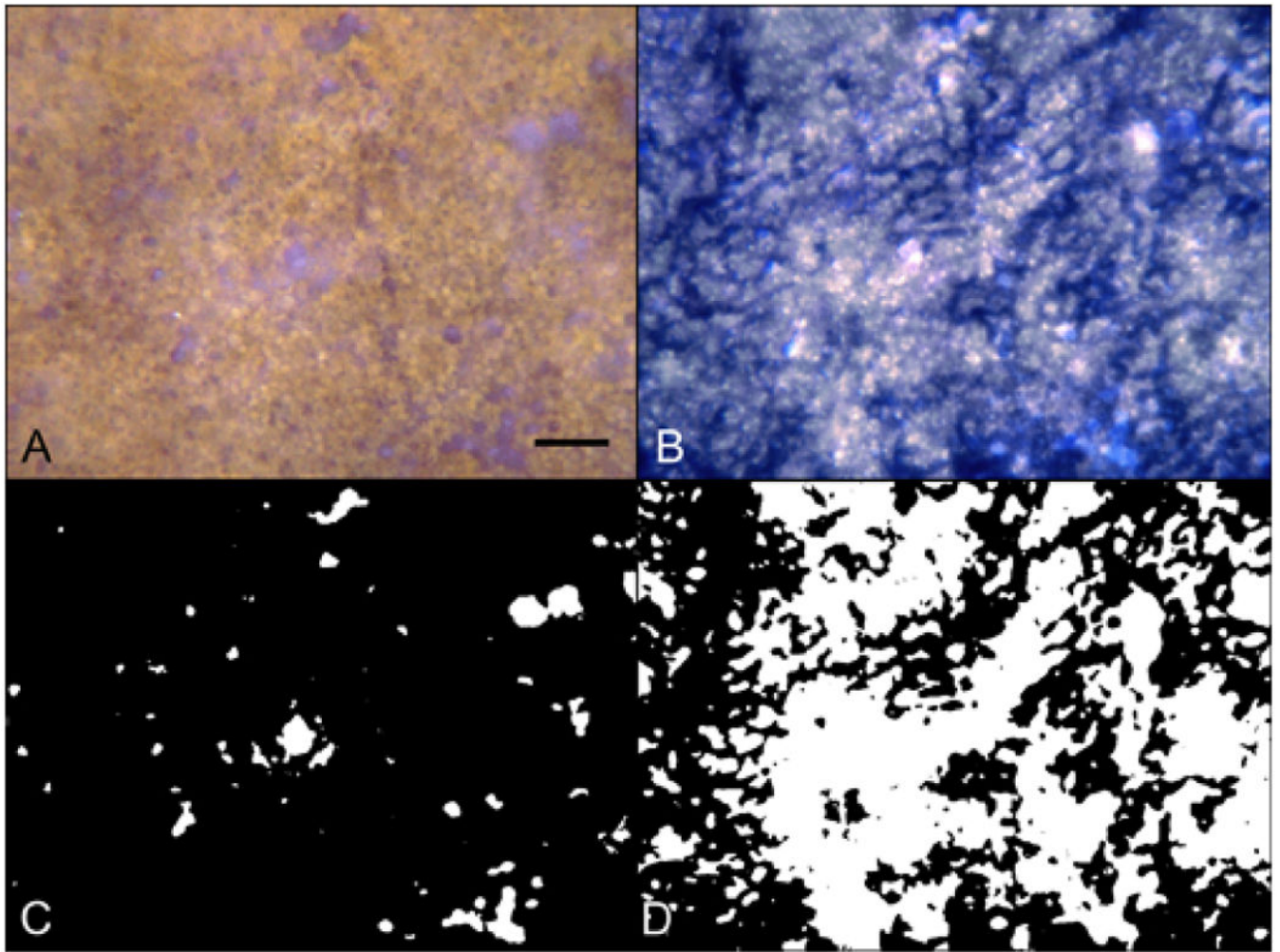
Figure 7.
Area from a 77 year-old Caucasian female with wet AMD (Case #11) 1 mm outside the CNV shown with epi-illumination (A) and transillumination (B) and the processed binary images used for percent RPE (C) and percent vascular area determinations (D). There are a few small areas of drusen and RPE defects present in the epi-illuminated images (A&C) while transmitted light images (B&D) show substantial loss of interconnecting capillary segments. (scale bar = 100 μm)
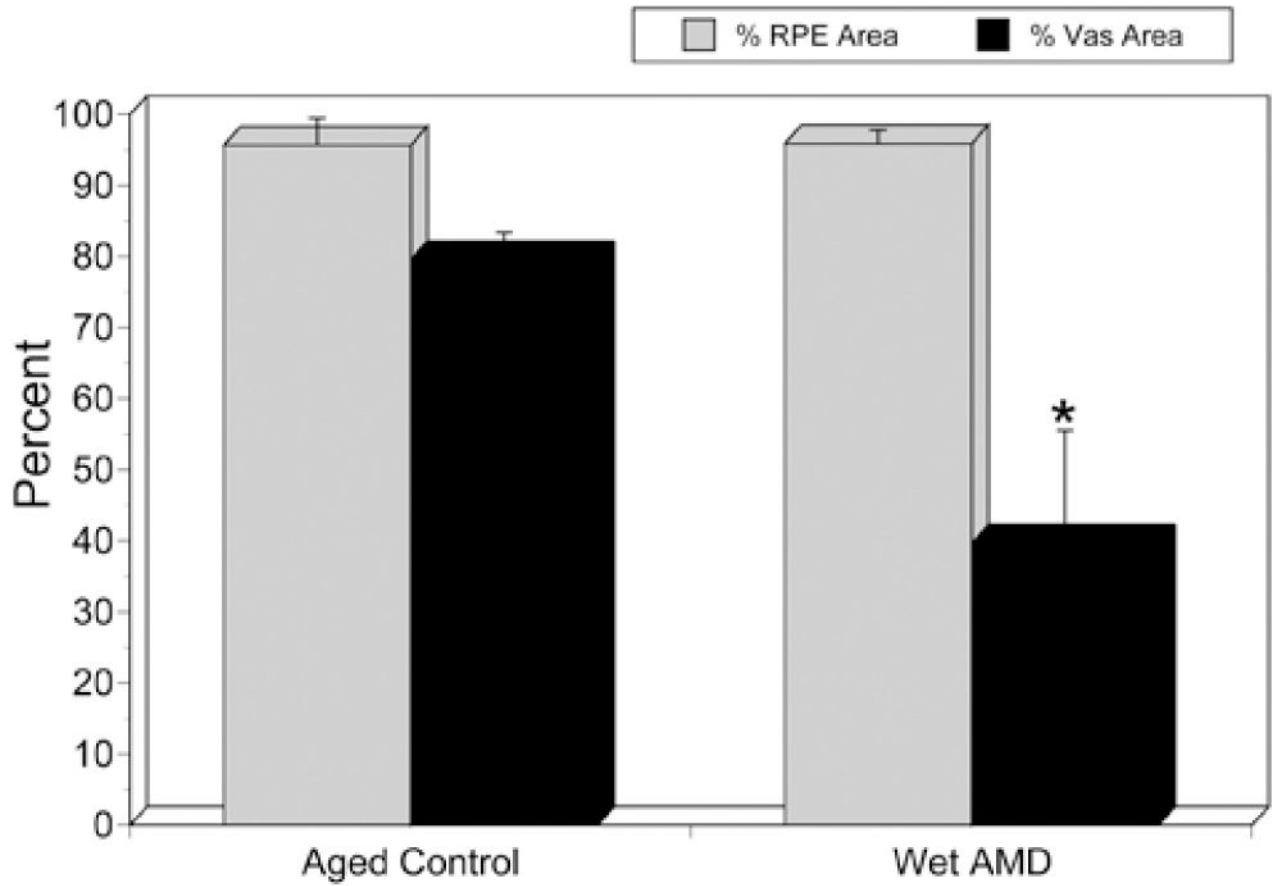
Figure 8.

Compared with aged control eyes, wet AMD eyes showed no significant difference in RPE area outside the area of CNV (P=0.845). However, the percent vascular area was significantly reduced (p=0.0096; asterisk).
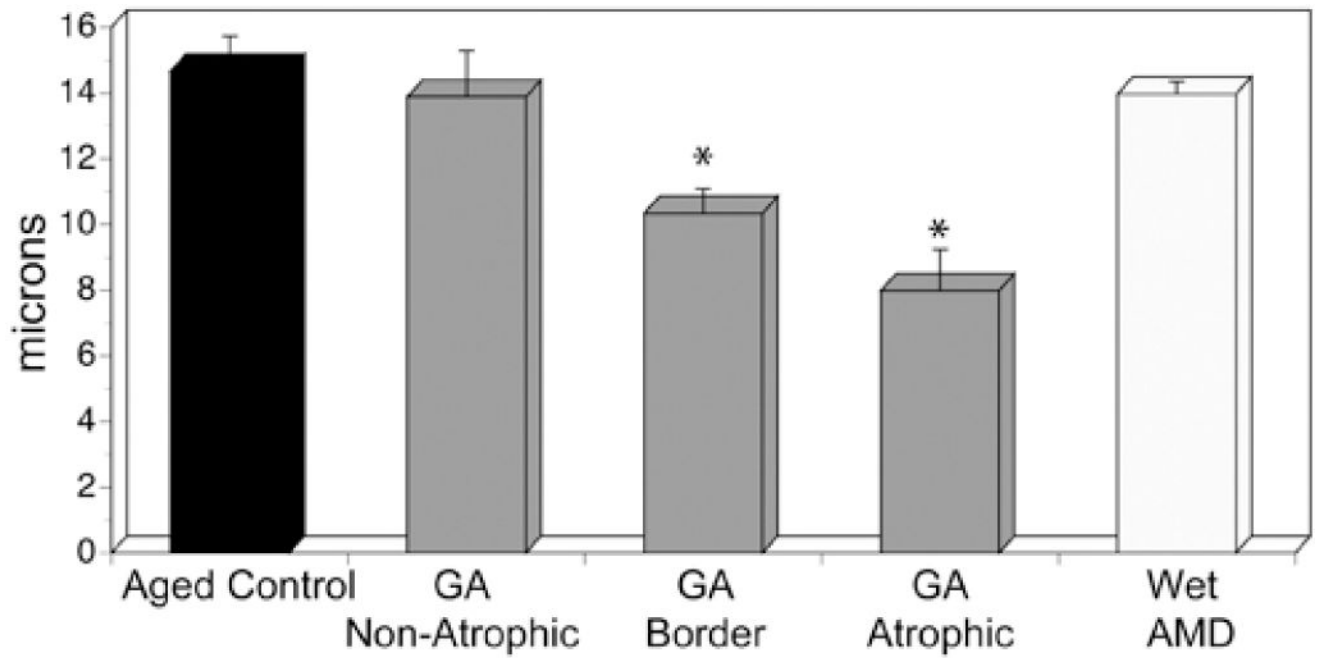
Figure 9.
There was no significant difference in choriocapillaris diameters between the aged control, the nonatrophic region of GA eyes and the wet AMD eyes. However, the choriocapillaris diameters were significantly less in the border regions compared to nonatrophic and in the atrophic regions compared to border regions in GA eyes.
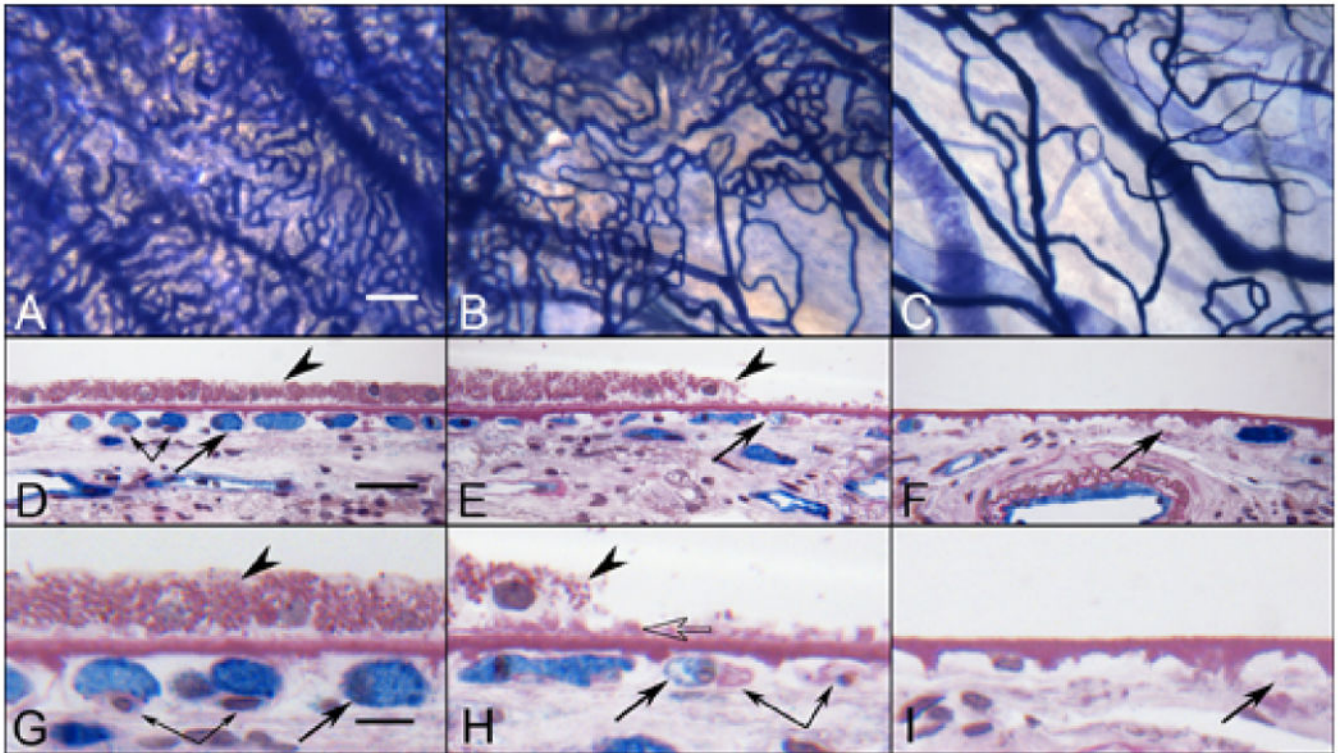
Figure 10.
APase choroid from a 88 year-old Caucasian male with GA (Case #9) showing the
nonatrophic region (A,D&G), border region (B,E&H) and atrophic region (C,F&I) in flat
view prior to embedment (A–C) and in cross sections stained with PAS and hematoxylin
(D–I). APase stained capillaries in the nonatrophic region (A) have broad diameter lumens
filled with serum APase (arrow in D&G), with endothelial cells and pericytes (paired
arrows) underlying viable RPE (arrowhead in D&G). At the border region, RPE appear
hypertrophic (arrowhead in E&H), capillaries appear constricted (arrow in E&H), and some
have completely degenerated (paired arrows H). A thin basal laminar deposit is associated
with Bruch's membrane (open arrow). In the atrophic region, many capillaries have
degenerated leaving only remnants of basement membrane material (arrows in F&I). Some
highly constricted viable capillaries had serum APase activity suggesting flow at some level.
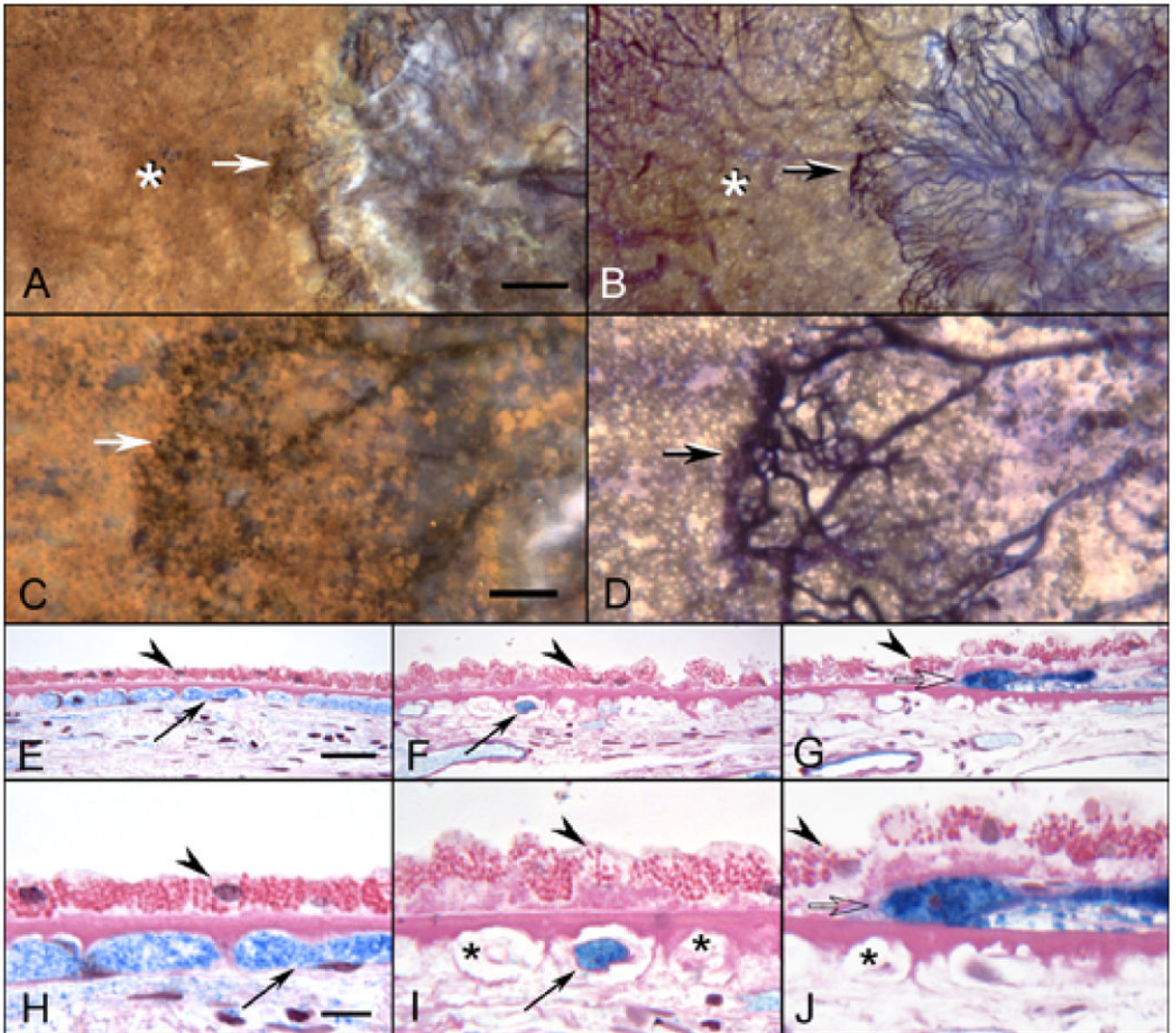(scale bar = 100 μm in A–C, 30 μm in D–F, 10 μm in G–I)

Figure 11.
APase choroid from an 81 year-old Caucasian female with wet AMD (Case #10) showing submacular CNV using epi-illumination (A&C) and transillumination (B&D). The front of growing vessels is closely associated with viable RPE (arrows A–D). Areas of CC dropout are evident in advance of the CNV (asterisks A&B). In PAS and hematoxylin stained sections, the equatorial region (E&H), has broad capillaries (arrows) containing serum APase with both endothelial cells and pericytes. The RPE has a normal morphology (arrowhead) and Bruch's membrane is free of deposits. In sections taken 1 mm beyond the CNV (F&I), only a few capillaries are viable (arrows) and many degenerative capillaries are seen (asterisks in I). The RPE is hypertrophic (arrowheads) and a basal laminar deposit is present. Sections taken through the edge of the CNV (G&J) show degenerative capillaries (asterisk in J), sub-RPE neovascularization (open arrow) and hypertrophic RPE overlying

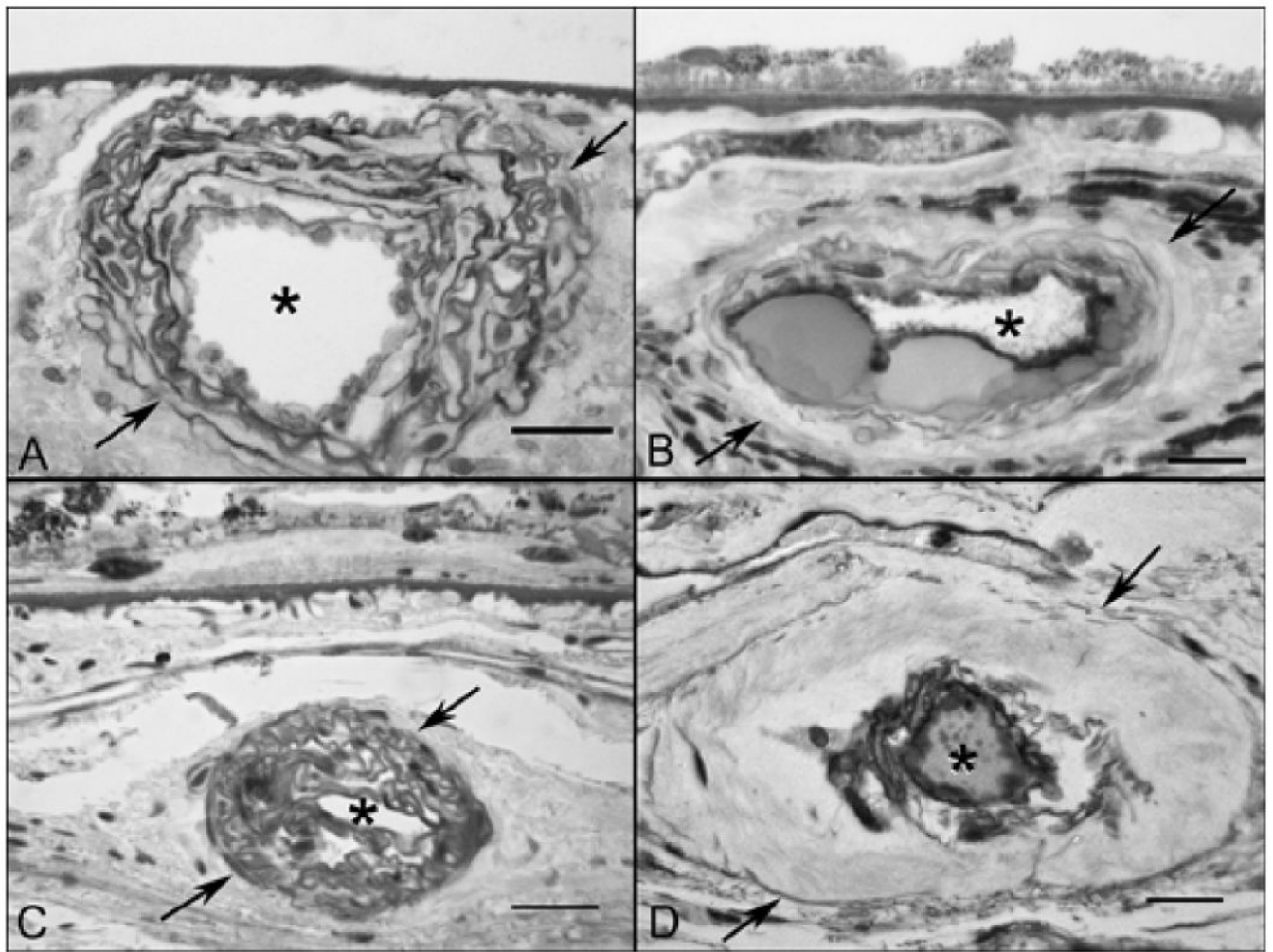the leading edge of the CNV. (scale bar = 0.5mm A&B, 100 μm C&D, 30 μm E–G, and 10 μm H–J)

Figure 12.
Arteriosclerotic changes shown in PAS and hematoxylin-stained sections from GA (A&B) and wet AMD subjects (C&D). (A) An artery in a GA subject (Case #5) showing hyperplastic changes consisting of concentric laminations of smooth muscle cells and basement membranes. (B) An artery in a GA subject (Case #4) showing formation of nodules that replace the media during hyalinosis. (C) Hyperplastic arteriosclerotic changes in a wet AMD subject (Case #10) and (D) hyaline arteriolosclerosis in a wet AMD subject (Case #9). (arrows indicate the outer vessel wall and asterisks indicate the lumen in all, scale bar = 20 μm in A, B & D and 30 μm in C)
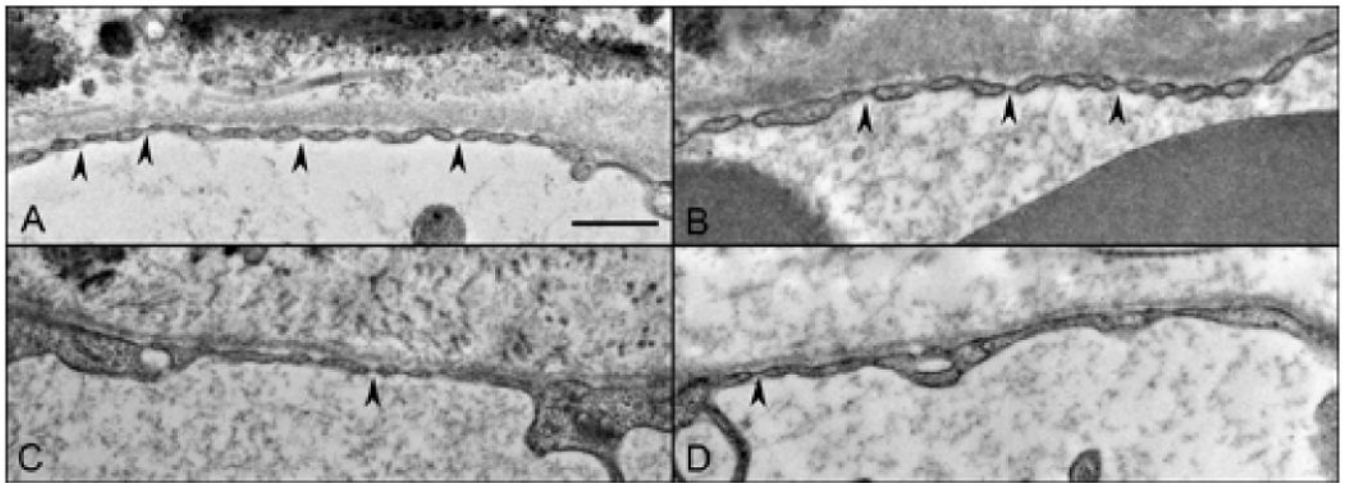
Figure 13.
Fenestrations (arrowheads) along the inner aspect of the choriocapillaris endothelium in an aged control eye (A), and in a GA eye where RPE were present (B), near the border region (C) and in the region of atrophy (D). (scale bar = 500nm)
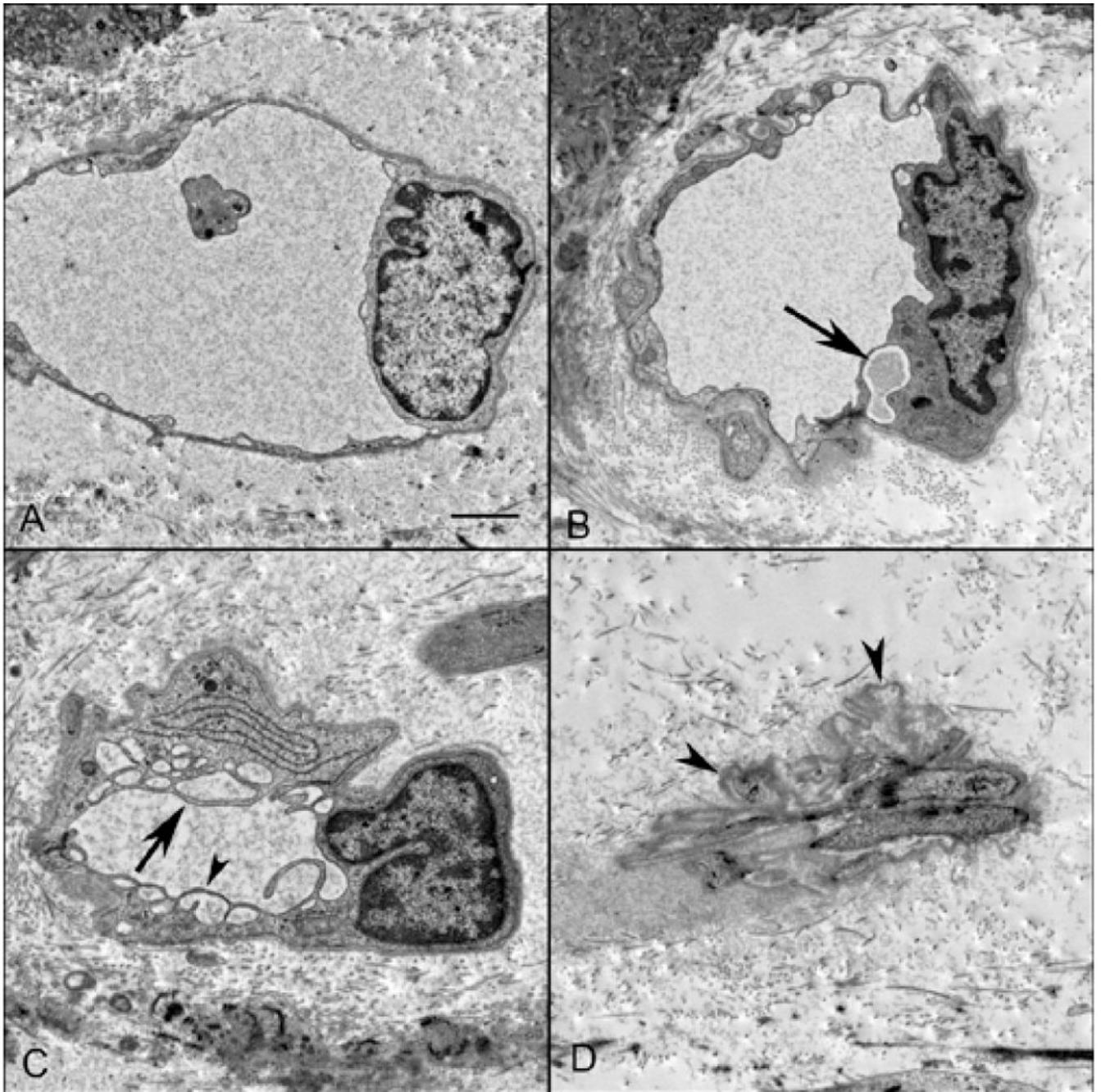
Figure 14.
Ultrastructure of choriocapillaris in a GA eye in TEM sections from a region with RPE (A), border region (B&C) and area of atrophy (D). Capillaries from the region with RPE had fine endothelial cell cytoplasmic processes surrounded by a thin basement membrane. Endothelial cells in capillaries from the border region (B) were often vacuolated (arrow) with thickened processes. Others were highly vacuolated with extensive cytoplasmic infoldings (C) that had fenestrations (arrowhead). In atrophic regions (D), degenerative

capillaries were collapsed and consisted almost entirely of basement membrane material (arrowheads). (scale bar = 1μm)

Table 1

Characteristics of human donor eyes

Case#	Time (hours) PMT	Time (hours) DET	Age/race/sex	Primary cause of death	Medical history	Ocular diagnosis
1	8	4	70/CM	Pulmonary embolism	HTN, Cancer	Aged Control
2	28	2.5	80/CM	COPD	COPD	Aged Control
3	31	4	84/CM	Cardiac arrhythmia	CAD	Aged Control
4*	9	2	84/CM	Lung Cancer	Cancer	GA
5	NA	NA	95/CM	Congestive heart failure	MI	GA
6	42	3.5	69/CF	Subarachnoid Hemorrhage	Pulmonary Fibrosis	GA
7*	9	6	88/CM	Congestive heart failure	CAD	GA
8	26	7.5	79/CM	COPD	CHF, CAD	GA
9	29	1	84/CF	Cardiac arrhythmia	CAD	Wet AMD
10	29	5	81/CF	Myocardial Infarction	HTN	Wet AMD
11	28	4	77/CF	GI Bleed	COPD, HTN	Wet AMD

DET – Death to enucleation time, PMT – Postmortem time (death to fixation), C – Caucasian, M – Male, F – Female, AMD– Age-related macular degeneration, DM – diabetes mellitus, HTN – Hypertension, COPD – chronic obstructive pulmonary disease, GA – Geographic atrophy, CAD-coronary artery disease, MI – Myocardial Infarction

NA- Not available

*
Patient followed clinically at Wilmer by Dr. Janet Sunness